# Differences in visual quality with orientation of a rotationally asymmetric bifocal intraocular lens design

Aiswaryah Radhakrishnan, MPhil, Carlos Dorronsoro, PhD, Susana Marcos, PhD

**PURPOSE:** To evaluate visual and perceptual performance for different orientations of a rotationally asymmetric bifocal intraocular lens (IOL) (M-Plus) simulated optically using a simultaneous vision simulator.

**SETTING:** Instituto de Optica, Madrid, Spain.

**DESIGN:** Prospective observational study.

**METHODS:** Perceptual quality and decimal high-contrast visual acuity (HCVA) was measured under cycloplegia for 8 orientations of the asymmetric bifocal IOL phase pattern at far, intermediate, and near distances simulated with a simultaneous vision simulator using face images and tumbling E targets. The preferred orientation at each distance was calculated as the centroid of the data for 8 orientations. The visual Strehl value was calculated using the subjects' ocular aberrations and multifocal pattern at each orientation. Optical predictions were obtained by implementing a differential visual Strehl values–based ideal observer model.

**RESULTS:** The study comprised 20 subjects (aged 21 to 62 years). Horizontal orientation (near segment at 0 or 180 degrees $\pm$ 45 [SD]) was preferred by 14 subjects and by 13 subjects at far and near distances, respectively; 8 subjects showed strong orientation preferences. The mean difference in preferred orientation between far and near was 27 $\pm$ 22 degrees. No significant differences in HCVA were observed. Optical predictions correlated strongly and significantly with measurements (far $r = 0.71$, near $r = 0.62$; $P < .0001$). The mean difference between measurement and simulation in the preferred orientation was 28 $\pm$ 29 degrees at far and 36 $\pm$ 28 degrees at near.

**CONCLUSIONS:** The perception varied for different orientations of an asymmetric bifocal IOL design tested using a simultaneous vision simulator. Optimum orientation was driven by interactions of the design with the eye's optical aberrations.

**Financial Disclosure:** None of the authors has a financial or proprietary interest in any material or method mentioned.

*J Cataract Refract Surg 2016; 42:1276–1287 © 2016 ASCRS and ESCRS*

Multifocal corrections are popular solutions for the treatment of presbyopia.[1] Clinical studies of multifocal intraocular lenses (IOLs) show improved near vision, generally at the expense of degradation of distance vision, compared with monofocal IOL corrections.[2] Refractive multifocal patterns devote discrete zones of the pupil to far vision and others for near (and sometimes also intermediate) vision. Computational[3] and experimental studies using adaptive optics[4] show that multifocal designs with a nonrotational (angular) distribution of zones and a lower number of far and near zones generally outperform designs with a higher number of zones and those with a radial zone distribution. In addition, a recent experimental study simulating angularly segmented bifocal corrections with a simultaneous vision simulator[A] showed the visual benefits for 2-zone angularly segmented designs compared with concentric or hybrid distributions. However, the rotationally asymmetric nature of the angular design and the orientation in which the IOL is implanted could affect visual performance.

 

http://dx.doi.org/10.1016/j.jcrs.2016.06.034
0886-3350

The M-Plus IOL (Oculentis, Inc.) is an angular-design IOL with 60% of the total lens area dedicated to far vision and 40% dedicated to near vision. Eyes with the angular-design IOL have functional vision similar to or better than eyes with other multifocal or accommodating IOLs.[5–8] Typically, angular-design IOLs are implanted with the near-vision zone placed inferiorly. A case report[9] showed that placing the IOL in a different orientation could be beneficial. In contrast, a recent study[10] found that on average, the orientation of the IOL does not significantly influence visual performance. Computational studies show that the ocular aberrometric profile[11] and the corneal comatic axis[12] of each patient might affect optical and visual outcomes with this angular-design IOL and that this interaction changes with the IOL orientation. Comparisons of visual perception and visual performance across IOL orientations in the same patients are hard to evaluate clinically because for any given patient, the IOLs are implanted at a single orientation.

Adaptive optics visual simulators are capable of simulating a multifocal correction, enabling a noninvasive systematic evaluation of multifocal designs for the same patient. Piers et al.[13] showed the expansion of the subjective depth of focus with spherical aberration induced by adaptive optics visual simulators, and de Gracia et al.[14] found that it occurred with certain combinations of astigmatism and coma. Vinas et al.[4] found differences in visual perception in normal subjects with simulated angular and radial segmented multifocal designs using a deformable mirror and spatial light modulator-based adaptive optics system. Using a simultaneous vision simulator, Dorronsoro et al.[A] showed that bifocal rotationally asymmetric designs tended to outperform other bifocal designs, although this differed across subjects. This simulator can be programmed for automatic simulation of different orientations of a multifocal IOL to evaluate the optical and neural interactions between the eye and the multifocal IOL design.

In this study, we used a purpose-designed simultaneous vision simulator provided with a spatial light modulator to test the influence of lens orientation of a rotationally asymmetric IOL design on perceived visual quality and visual acuity at different distances in patients with paralyzed accommodation.

## SUBJECTS AND METHODS

The measurement protocols met the tenets of the Declaration of Helsinki and were approved by the review board of Consejo Superior de Investigaciones Cientificas, Madrid, Spain. All subjects provided a written informed consent.

All measurements were performed with paralysis of accommodation and therefore under simulated presbyopia. Cycloplegia was induced with tropicamide 1.0% (3 drops at 5-minute intervals, 15 minutes before taking the measurements, and then 1 drop every hour thereafter).

### Simultaneous Vision Setup

A purpose-designed simultaneous vision simulator (Figure 1) was used to simulate angular bifocal corrections and to perform psychophysical evaluations at 3 distances. The system has been described in detail.[15,16,A,B] In brief, 2 channels provided with 2 Badal systems separated by 2 beam splitters recombine at a pupil plane, thereby allowing the defocus to be changed independently. One channel is focused at far, whereas the other channel introduces a near-vision addition that can be changed continuously. A digital light projector (DLP, Texas Instruments, Inc.) with a resolution of 800 pixels × 600 pixels projects visual stimuli that are viewed simultaneously through both channels. In a modified version of the instrument,[B] a transmission spatial light modulator is placed in a pupil conjugate plane with a linear polarizer. These efficiently simulate phase patterns, as shown by the good correspondence between visual perception with physical multifocal pattern lenses and reflection spatial light modulator simulations of those patterns.[17,A–C] Two orthogonally oriented linear polarizers placed in the Badal channels projects near-focused or far-focused images, following the black and white pupillary masks displayed in the spatial light modulator. Figure 1 shows the current configuration of the system. The effective luminance of the test stimulus was 39 candelas (cd)/$m^2$. The test stimulus and pupil mask presentation were synchronized in Matlab using the Psychtoolbox.[18]

In this study, the focus difference between the 2 channels was set to +3.0 D. Far vision was simulated by placing the far channel (Badal 2) at best focus and the near channel (Badal 1) at best focus +3.0 D. Near vision was simulated by placing Badal 2 at best focus −3.0 D and Badal 1 at best focus. Intermediate vision was simulated by placing Badal 2 at best focus −1.5 D and Badal 1 at best focus +1.5 D. All

Submitted: March 14, 2016.
Final revision submitted: June 6, 2016.
Accepted: June 17, 2016.

From the Laboratory of Visual Optics and Biophotonics, Instituto de Óptica Daza de Valdés, Consejo Superior de Investigaciones Científicas, Madrid, Spain.

Funding provided by the European Research Council under the European Union's Seventh Framework Programme (FP7/2007-2013)/ERC Grant Agreement number 294099 (Dr. Marcos), Spanish Government grant FIS2011-264605 and FIS2014-56643-R (Dr. Marcos), the 7th Framework Programme of the European Community through the Marie Curie Initial Training Network OpAL (OpAL is an Initial Training Network funded by the European Commission under the Seventh Framework Programme), (PITN-GA-2010-264605, Dr. Radhakrishnan), and Oculentis GmBH, Germany.

Corresponding author: Aiswaryah Radhakrishnan, MPhil, Visual Optics and Biophotonics Laboratory, Instituto de Optica, Consejo Superior de Investigaciones Científicas, Serrano, 121, Madrid 28006, Spain. E-mail: aishu@io.cfmac.csic.es.

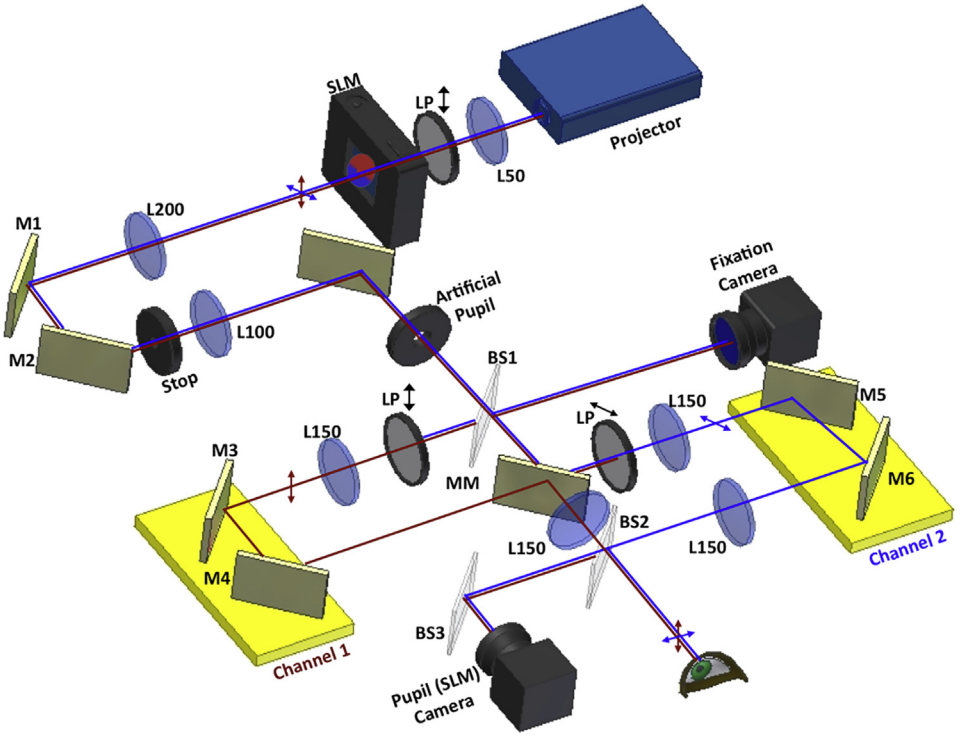


**Figure 1.** Schematic diagram of the modified simultaneous vision simulator (BS = beam splitter; L = lens; LP = linear polarizer; M = mirror; MM = double mirror; SLM = spatial light modulator).

measurements were performed for 5.0 mm pupil diameters, which are maintained by the masks placed in the spatial light modulator.

## Simulation of the Rotationally Asymmetric Intraocular Lens

The M-Plus,[19] an angular profile IOL with a small radial zone at the center for far vision, was simulated. The far-to-near energy ratio was 60:40. Masks were created using Matlab, consisting of white and black portions of a circular image (5.0 mm diameter) representing far-vision and near-vision zones, respectively. Figure 2, *A*, shows an example of the mask and its optical representation at the pupillary plane. These patterns are programmed in the spatial light modulator and presented at 8 orientations of the mask. The angular notation (Figure 2, *B*) represents the orientation of the near zone. For convention, the right-eye data are flipped horizontally[20] so that 0 degree represents the nasal orientation in right eyes and left eyes.

## Perceptual Scoring

Subjects viewed 2-degree visual field face images (Figure 3, *top*) displayed by the digital light projector through the 8 orientations of the bifocal design presented in random order interspersed with a gray field (Figure 3, *middle*). For each presentation, the subject graded the image on a 6-score grading scale from very blurred (−10), blurred (−5), not so blurred (−1), not so sharp (1), sharp (5), and very sharp (10) using keyboard inputs. Figure 3 shows an example of the scoring by 1 subject on a particular series of presentations. The measurement was repeated 10 times, and the mean score for each orientation was calculated and taken as the perceptual score.[4,21] The presentation of the test image and pupil

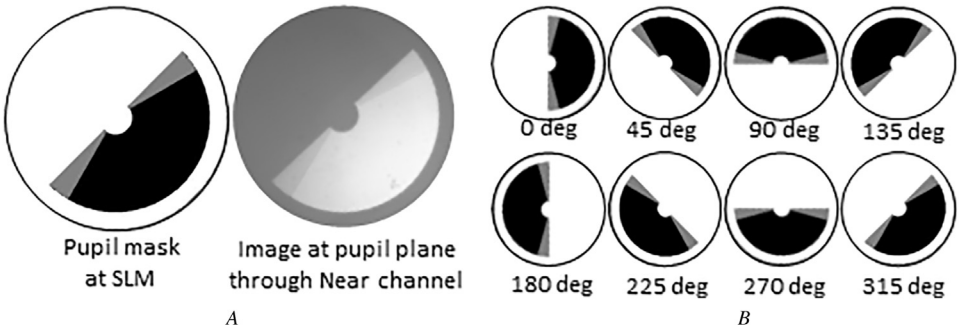


**Figure 2.** Grayscale patterns programmed in the spatial light modulator, representing the angular-design IOL. *A*: Programmed grayscale image (*left*) and pupillary plane image captured on a charge-coupled device placed at the eye's pupillary plane. *B*: Grayscale patterns programmed at different orientations. White segments correspond to the far-vision zone, black segment corresponds to near-vision zones, and the gray region corresponds to the transition zones (deg = degrees; SLM = spatial light modulator).

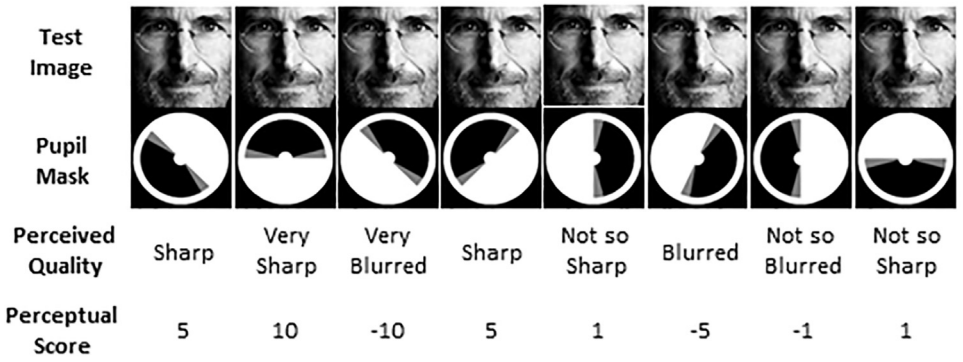


**Figure 3.** Illustration of a perceptual scoring setting for 1 subject on 1 face image (*top*) viewed through 8 rotated patterns (*middle*). Scores ranged from −10 (very blurred) to + 10 (very sharp) (*bottom*).

mask and the acquisition of the response were synchronized using Matlab.

## Orientation Preference

For testing the orientation preference (Figure 4), subjects subsequently viewed a face image (2-degree field) through 2 pairs of random orientation bifocal patterns. Each image was viewed for 1.5 seconds, with a gray screen presented between each image pair presentation. The subject's task was to choose the better focused image (first or second) of the pair and indicate the confidence of choice on a 3-level confidence scale. Each session consisted of the presentation of 36 random pairs, and the measurements were repeated 10 times.

## Decimal Visual Acuity Measurements

Decimal visual acuity (logMAR = −log10 [decimal acuity])[22] was measured using white E letters on a black background that was presented in 8 random orientations of varying sizes (Figure 5). At the beginning of the trial, an E target of suprathreshold size and a random orientation was presented. The task of the subject was to identify the orientation of the E letter and respond using a keyboard (8AFC). The size of E in the subsequent presentation was decreased or increased depending on the subject's response using a quaternion estimation algorithm.[23] The presentation orientation was randomized. A run consisted of 50 trials and 20 reversals, and the visual acuity was measured as the mean of the last 10 reversals. The measurements were repeated for all 8 orientations of the bifocal pattern and for far, intermediate, and near distances.

## Aberrometry Measurements

The ocular aberrations were measured using a Shack-Hartmann aberrometer (HASO32, Imagine Eyes, Inc.), which is part of a purpose-designed adaptive optics system.[24] Measurements were performed under cycloplegia. Defocus was corrected using a Badal optometer while the subject fixated on a 2-degree white Maltese cross on a black background. The pupil diameter was limited to 5.0 mm using an artificial pupil placed at a pupil conjugate plane.

## Optical Simulations

The pattern orientation preference was simulated using an ideal observer model whose responses to an orientation preference task (similar to the subjective task) are based on the visual Strehl metric.[25] For each subject, the through-focus visual Strehl was computed for wavefront aberration resulting from the combination of the measured subject's ocular aberrations (astigmatism + higher-order aberrations [HOAs]) and the bifocal patterns at each orientation. In all subjects and for all distances (best focus at +1.5 D and at +3.0 D), a differential visual Strehl value for each orientation was compared with that for all other orientations. Scores of 10, 5, and 1 were assigned when the differences were above 75%, 50%, and 25% thresholds, respectively, corresponding to the monofocal visual Strehl value at that distance.

## Data Analysis

Perceptual and optical preference measurements were analyzed similarly. Weights were assigned to the positive response (images selected as the better of the pair) and negative responses (images not selected) according to the confidence of the response (from +10 to +1 and from −10 to −1). The scores assigned to each pattern orientation were summed, and a sum-weighted preference score was obtained. A polar plot was generated from the scores at each orientation, and the centroid of the corresponding polar curve was calculated for each distance. The orientation of the centroid indicates the preferred orientation, and the radius indicates the strength of the preference. For identifying significant preferences, Bernoulli statistics were used. A score greater than +15 for a given orientation was


**Figure 4.** Illustration of the pattern preference of the psychophysical paradigm (s = seconds).

**Figure 5.** Decimal visual acuity measurement using E optotypes in 8 orientations.

considered significant, indicating that the orientation produced significantly better optical or visual performance.

## RESULTS

The study comprised 20 subjects aged 21 to 62 years with refractive errors from +2.50 to −5.50 diopters (D) and astigmatism less than 1.00 D. Eight subjects did not have previous experience performing psychophysical experiments.

### Changes in Perceptual Score with Pattern Orientation

Figure 6 shows the perceptual score for different orientations across different distances as a polar plot. The center of the plot corresponds to a score of −10 and the outer line corresponds to +10 symmetrically in all orientations. Data for far are indicated in red, intermediate in green, and near in blue. The mean perceptual score across subjects did not vary across orientations or distances (Figure 6, *A*), although the curves tended to elongate for 0 degrees and 180 degrees. However, there were high intersubject variabilities in this performance. Figure 6, *B* to *D*, shows the perceptual score plots for 3 subjects. For example, for subject 2, the perceptual score was highest for 180 degrees at far, and for 270 degrees at intermediate and near. For the other 2 subjects (S11 and S18), the score was highest at 0 degrees for both far and near and 0 degrees and 90 degrees for far and near, respectively.

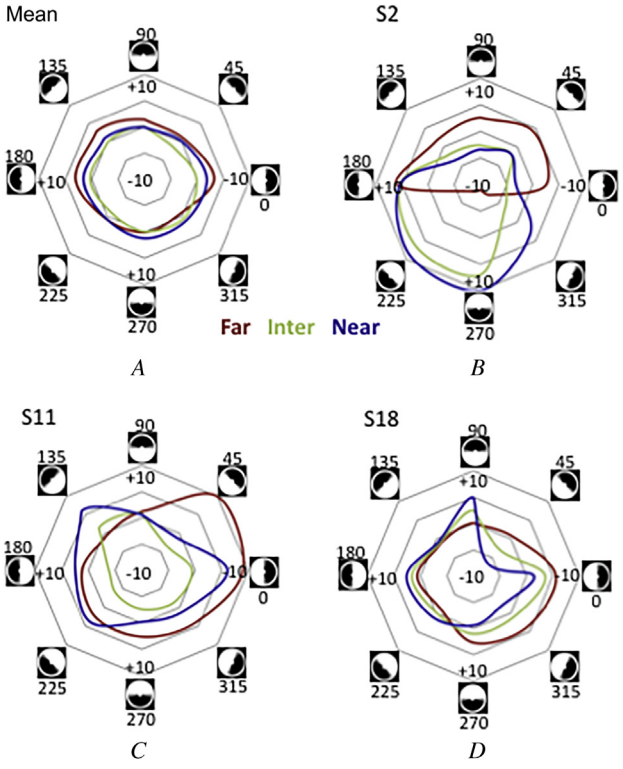


**Figure 6.** Perceptual score across orientations at far (*red*), intermediate (*green*), and near (*blue*) distances. *A*: Mean perceptual score. *B* to *D*: Examples of subjects (Inter = intermediate; S = subject).

The overall perceived image quality across orientations at any distance was calculated as the area of the circle formed by the perceptual scores at the given distance. The mean score was 5.6 ± 1.2 (SD) at far, 2.1 ± 1.07 at intermediate, and 4.1 ± 1.05 at near. The mean difference in perceived image quality (score) between far and near was 2.5 ± 1.4 and was not significant ($P = .37$).

### Orientation Preference

Figure 7 shows the weighted preference with the respective centroids for all subjects. The center of the plot corresponds to a preference score of −100 and extends symmetrically across all orientations to a score of +100. The arrows indicate the orientation of the centroid (preferred orientation), and the length of the vector indicates the strength of preference. The weighted perceptual preferences (experiment 2) correlated significantly with the perceptual score (experiment 1) across all subjects and distances ($r = 0.48$, $P = .004$). At far, 6 subjects preferred nasal quadrant orientations (0.0 ± 44.5 degrees), 4 subjects preferred superior quadrant orientations (90.0 ± 44.5 degrees), 8 subjects preferred temporal quadrant orientations (180.0 ± 44.5 degrees), and 2 subjects preferred inferior quadrant orientations (270.0 ± 44.5 degrees). At near, 8 subjects preferred nasal quadrant orientations, 5 subjects preferred temporal quadrant orientations, 6 subjects preferred inferior quadrant orientations, and 1 subject preferred superior quadrant orientations.

Figure 8 shows the centroid locations for far (*filled symbols*) and near (*open symbols*). Values outside the inner circle (radius of 15) are significant. Eight subjects had a strong orientation preference at far and

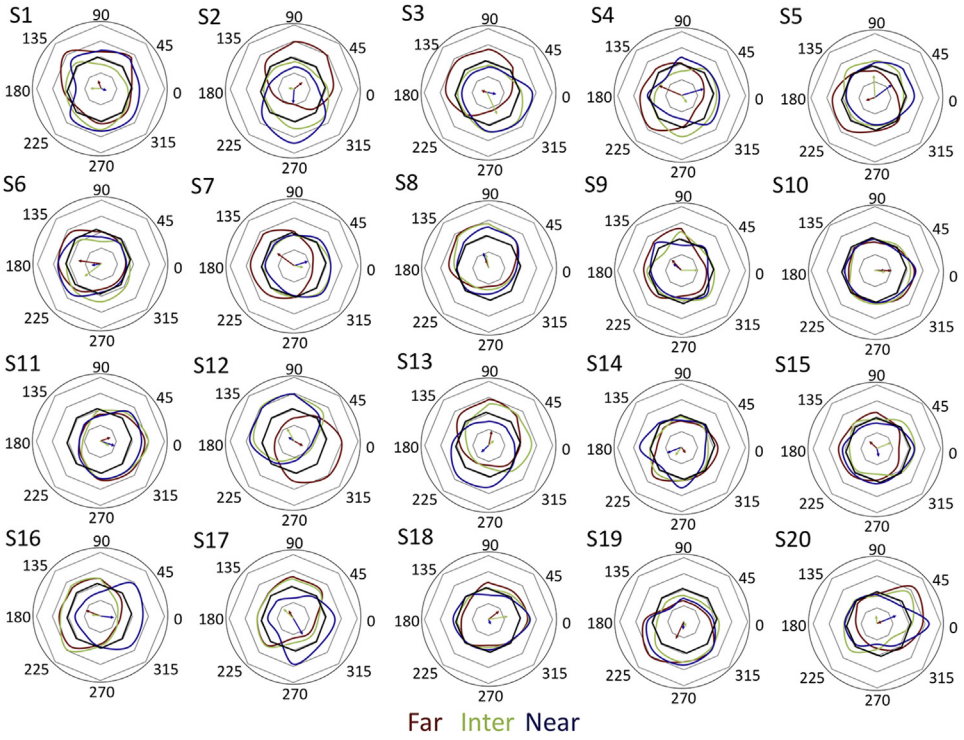


**Figure 7.** Weighted orientation preference for all subjects at far (*red*), intermediate (*green*), and near (*blue*) distances. At any orientation, the axes extend from +100 to −100 in the center, with the black line representing zero. Arrows indicate the preferred orientation at the respective distances, with the length of the arrow indicating significant preferences (S = subject).

9 subjects had strong orientation preference at near. The mean angular difference in the centroid orientation between far and near was 27 ± 22 degrees and correlated significantly ($r = 0.32$, $P < .05$), indicating that in most subjects the orientation preference was retained across distances.

## Changes in Decimal Visual Acuity

The mean decimal visual acuity across subjects and orientations was 0.63 ± 0.02 D at far and 0.556 ± 0.021 D at near. This corresponds to 1 line difference in visual acuity with conventional charts. As shown in Figure 9, the visual acuity did not vary much across orientations at any distance. The maximum difference in the mean visual acuity across any 2 orientations at far, intermediate, and near was 0.06, 0.11, and 0.05, respectively.

## Ideal Observer Model

The responses of an ideal observer model were based on the visual Strehl values at the measured distances. In a diffraction-limited eye, through-focus visual Strehl curves are the same for all orientations (Figure 10, *A*). In real eyes, the amplitude and overall shape of the through-focus curves might vary across orientations; Figure 10, *B*, shows an example for

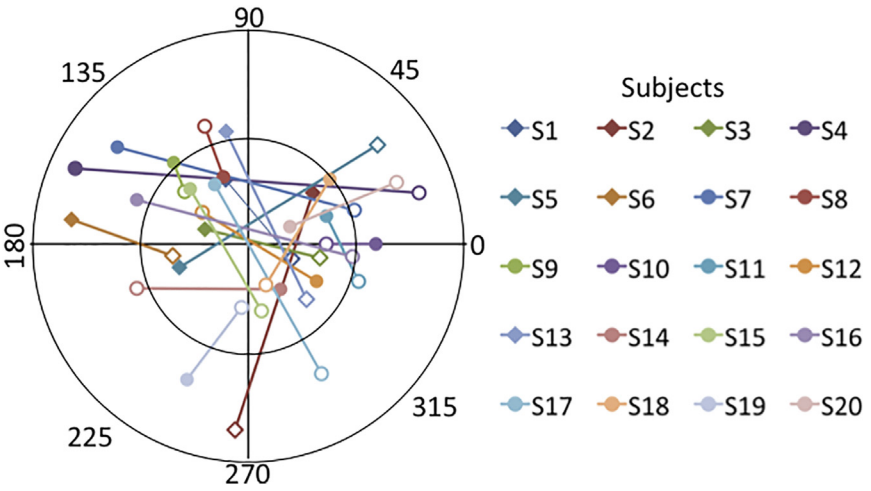


**Figure 8.** Centroid locations of the weighted orientation preference plots for all subjects. Filled symbols represent centroid locations for far, and open symbols centroid locations for near. The inner circle represents the limit for statistical significance (ie, values outside the circle are significant).

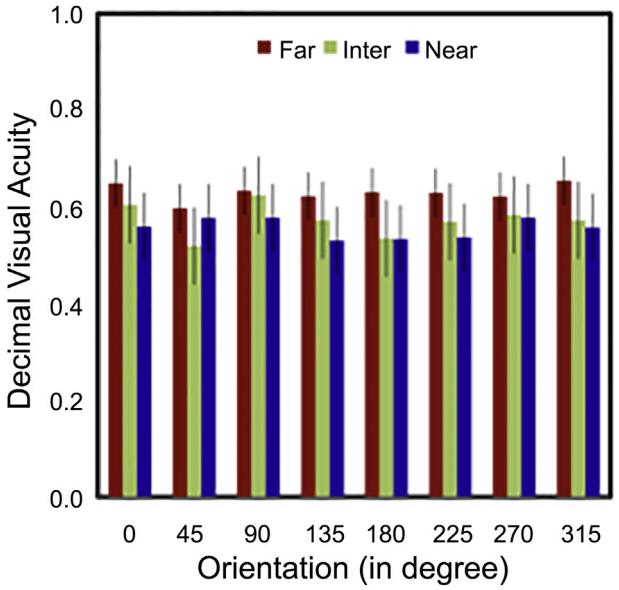


**Figure 9.** Average decimal visual acuity at different orientations across subjects at far (*red*), intermediate (*green*), and near (*blue*) distances (Inter = intermediate).

subject 2. Figure 11 shows the orientation preferences of each subject using the ideal observer model, which responds based on visual Strehl values. As in the perceptual orientation preference plots (Figure 7), the center of the plot corresponds to the optical preference score of −100 and extends symmetrically across all orientations to a score of +100. The arrows indicate the orientation of the centroid (preferred orientation), and the length of the vector indicates the strength of preference. The simulated optical preference plots and the perceptual preference plots correlated significantly with the measured data at far and near distances (far, $r = 0.71$, near $r = 0.62$; $P < .0001$), although not for intermediate distances ($r = -0.021$, $P = .87$). A Bland-Altman analysis found good agreement (better for far distance) between measurements and simulations at all distances (far $P = .46$, intermediate $P = .19$, and near $P = .24$).

Figure 12, *A* to *C*, shows the centroid locations of the perceptual preference (*filled symbols*) and optical simulated preference (*open symbols*) polar plots for far, intermediate, and near distances. In general, there was a high correspondence between perceptual and optical centroid locations for far (28 ± 29 degrees) and for near (36 ± 28 degrees) distances, with the data falling in the same quadrant except for the intermediate distances (80 ± 63 degrees). There was a strong significant correlation (Figure 13) between the perceptual centroids and optical centroids at far and near distances (far $r = 0.89$, near $r = 0.94$; $P < .0001$). Even at the intermediate distance, a weak correlation was observed (intermediate $r = 0.47$, $P < .05$). The radius of the centroid estimated from optical simulations was higher than it was from the perceptual measurements in 13 subjects (65%) across distances, probably resulting from discrepancies in the perceptual weighting by the subject and the ideal observer. Across distances and subjects, the mean difference in radius between the simulations and measurements was 1.8 ± 7.8 and did not correlate significantly at any distance.

## DISCUSSION

We systematically evaluated the perceptual and visual performance differences using the orientation of a rotationally asymmetric bifocal pattern (mimicking the angular-design IOL M-Plus) simulated in a simultaneous vision simulator. Although visual acuity did not change significantly, the perceptual score showed a clear bias toward specific orientations. The perceptual orientation preferences varied across subjects and in some cases, across distances. These preferences were determined mostly by the optical interactions of the eye's optical aberrations and the bifocal pattern.

Multifocal IOL implantation is aimed at providing patients with good uncorrected visual acuity for both

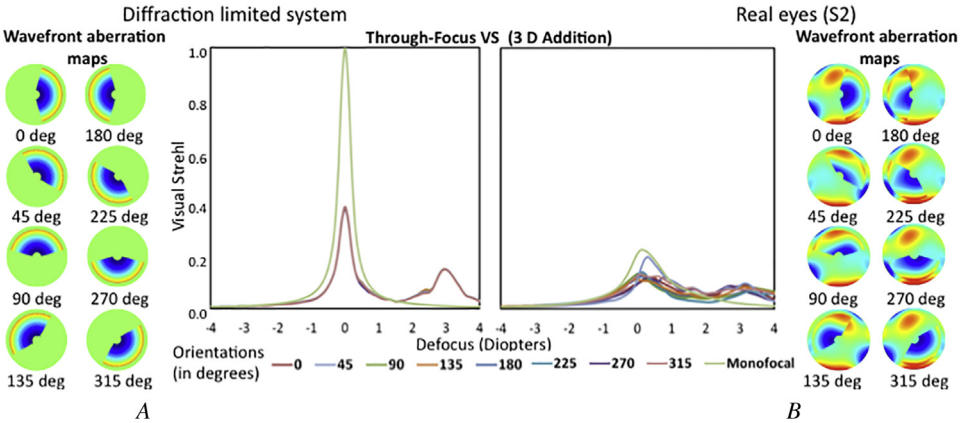


**Figure 10.** Wave aberrations and through-focus visual Strehl for 8 orientations for (*A*) a diffraction-limited eye and (*B*) a patient's eye with real aberrations (S2) (deg = degrees).

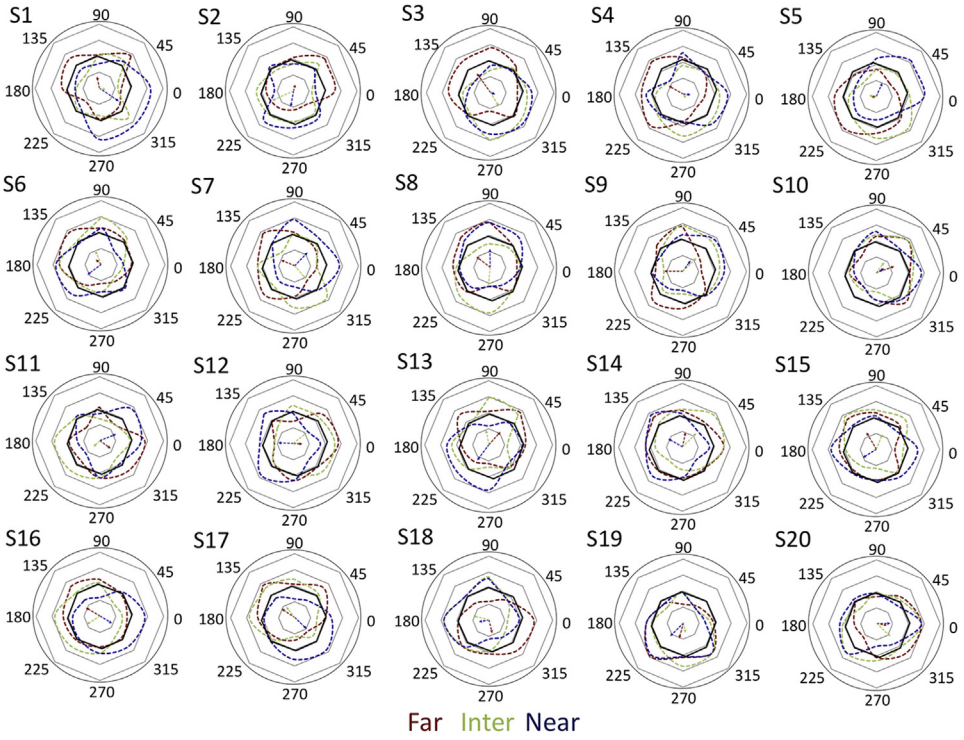


**Figure 11.** Simulated weighted orientation preference for far (*red*), intermediate (*green*), and near (*blue*) distances for all subjects. The axes extend from +100 to −100 in the center, with the black line representing the zero. Dashed arrows indicate the preferred orientation at the respective distances, with the length of the arrow indicating significant preferences (Inter = intermediate; S = subject).

distance and near visual tasks. The bifocal design we tested provided high-contrast visual acuity (HCVA) at the far and near distances in the near normal visual acuity range. The bifocal design was distance dominant and concurrent to the bifocal design; the visual acuity at near was more than 1 line lower than the distance visual acuity. The visual acuity reported in our study was within the range of visual acuities reported in previous studies.[2] Despite the absence of a correction at the intermediate region, the visual acuity was relatively well preserved at intermediate distance.

The decimal HCVA was unaffected by the orientation of the angular bifocal design. It is likely that the differences across orientations are not apparent with high-contrast stimuli, although these differences could have been present in low-contrast visual acuity.[26,27] In other words, conventional tests for visual acuity appear to be insensitive to changes introduced by blur orientation and might not be useful indicators of the preferred IOL orientation.

Changes in perceived image quality at different orientations from both perceptual measurements (perceptual scoring and perceptual preference) were concurrent in most subjects. Twelve of the 20 subjects had a significant correlation between perceptual scores and weighted perceptual scores for far distance across all orientations, and for only 2 subjects were these uncorrelated or negatively correlated. Similar to the visual acuity results, the overall perceptual quality was better at far than at near and was worse for

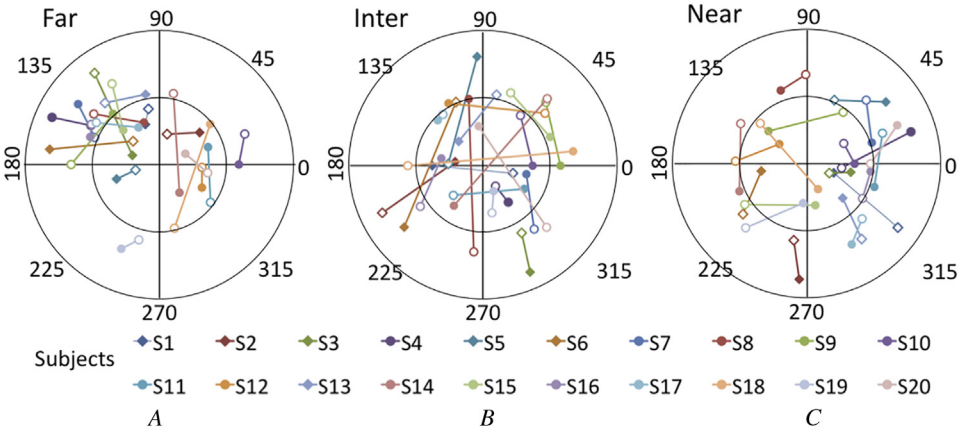


**Figure 12.** Centroid locations from perceptual measurements (*filled symbols*) and optical simulations (*open symbols*) data at (*A*) far, (*B*) intermediate, and (*C*) near distances for all subjects. The inner circle represents significant radius of centroids (Inter = intermediate; S = subject).

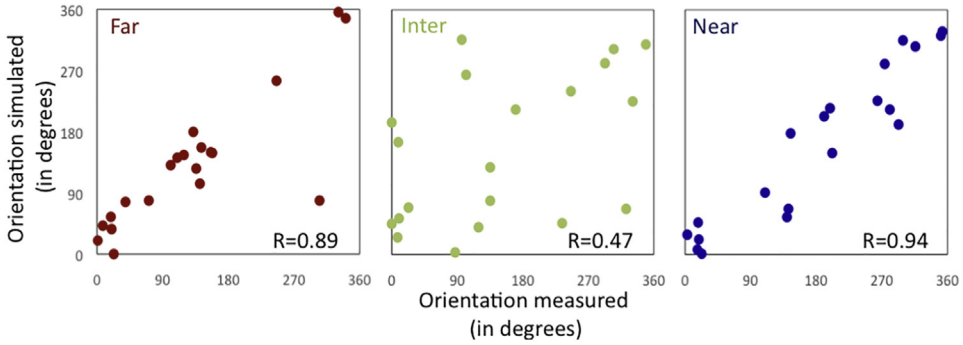


**Figure 13.** Correlations of the weighted orientation preference plot centroid angular coordinates (optimum orientation) from perceptual measurements and optical simulations for far, intermediate, and near distances (Inter = intermediate).

intermediate acuity. However, the IOL design simulated was bifocal (60 far/40 near) and had no energy dedicated to the intermediate zone. The residual optical quality at intermediate is likely to have resulted from the interaction between the ocular aberrations of each subject and the peak foci. In addition, measurements were performed for a fixed pupil diameter of 5.0 mm. The angular nature of the IOL design makes performance less dependent on pupil diameter.[19] A 5.0 mm pupil diameter was chosen to correspond with the typical average pupil diameter for a luminance of 44 cd/m$^2$ in a presbyopic population (aged 40 to 60 years)[28] and as the pupil diameter for which the optical performance of the M-Plus angular-design IOL has been characterized on bench testing.[19] The angular nature of the design makes performance less dependent on pupil diameter.[19] Although modifying the pupil diameter will modify the amount of aberrations and the interactions of the aberrations with the IOL, we do not believe these differences would affect the general trends.

On average, the orientation preferences showed a trend toward the horizontal axis, although the orientation bias differed across subjects. The conventional orientation of IOL implantation in the clinic is with the near zone at 270 degrees; however, only 1 subject showed consistent preferences to this orientation at all distances. Many subjects showed a preference along the horizontal axis for far and near distances in the perceptual score and orientation preference measurements, although the vertical orientation was favored more often at near distance. This bias could have an optical or neural origin.

Orientation tuning in the visual system,[29,30] especially to horizontally oriented targets,[30,31] has been reported. Ohlendorf et al.[31] showed that subjects could tolerate horizontally oriented astigmatism better than vertically oriented astigmatism. Vinas et al.[32] found lower visual degradation with induced horizontal astigmatism than with astigmatism induced vertically or obliquely. Long-term bias to oriented blur has been shown to persist even after long-term wear of corrective astigmatic lenses.[33] Although it has been shown that subjects are adapted to their own aberration orientation,[34] it has also been shown that subjects can adapt to a new aberration pattern/blur orientation[35] and even to pure simultaneous vision blur.[21] Whether subjects can adapt to new oriented blur produced by a rotationally asymmetric IOL remains to be evaluated.

The perceptual preference to orientation showed distinct trends between groups of subjects. Although some subjects showed consistent and strong orientation preferences across distances, few subjects showed strong preferences that varied across distance and few subjects had no significant orientation preferences. Across all subjects, the strength of preference was reduced even though the preferred orientation was along the horizontal axis, indicating that these preferences are highly subjective and should be treated on an individual basis. This finding explains why in a study by de Wit et al.,[10] a bias was not apparent as a group trend in patients who had the M-Plus angular-design IOL implanted in different orientations.

Orientation preferences were simulated using an ideal observer model generated from the through-focus visual Strehl value calculated from the ocular aberration measurements at best focus. Good agreement was found between optical simulations and the perceptual measurements (far $r = 0.89$, near $r = 0.94$; $P < .0001$). In fact at far, the preferred orientation estimated from perceptual measurements was within $\pm 45$ degrees (smallest step of rotation measured in the study) of the preferred orientation obtained from simulations in 90% of the subjects. On the other hand, 40% of the subjects still had a difference of less than 20 degrees (clinically relevant) between the simulated orientation and the measured preferred orientation. These results suggest that the orientation bias is strongly influenced by the ocular optics. Most subjects in this study had coma-like aberrations oriented along the oblique axis, which was reflected in the orientation preferences.[12]

The optical simulations were performed using the visual Strehl value as a metric, which exclusively represents optical contrast differences across orientations.

It is conceivable that a metric that also considers the orientation of the retinal blur (produced by each combination of ocular aberration and bifocal pattern orientation) rather than the overall contrast only might improve the predictions. Given the good prediction of the orientation bias on optical grounds it is conceivable that the best selection of IOL orientation can be planned based on optical aberrations. In any case, a full account of the optics and neural aspects can be achieved by using a simultaneous vision simulator or adaptive optics visual simulators.

This study shows that choosing the optimum orientation of a rotationally asymmetric IOL might help improve the visual performance of these IOLs. Several subjects showed clear preferences for a particular orientation, which was the same at far, intermediate, and near distances; few other subjects showed no typical tendencies with orientation at any distance. These are probably the most ideal subjects for the implantation of angularly segmented multifocal IOLs. On the other hand, over one third of the subjects had a different preferred orientation for far and near distances. The orientation of IOL implantation in these cases might depend on the subject's visual needs or might be based on the preferences at far. Some of the subjects had strong preferences to orientation, which further stresses the importance of an orientation preference assessment before the surgical intervention.

A natural follow-up to the study could entail potential changes in the orientation preference after adaptation to a nonpreferred orientation. In previous studies, we found short-term adaptation effects after exposure to pure simultaneous vision, to other aberration patterns, and to oriented blur, suggesting that adaptation to an initially nonpreferred orientation might happen.

In this study, the rotation accuracy necessary for this optimization could only be speculated on because our perceptual measurements were performed in 45-degree increments and the mean difference between the predicted best orientation and that estimated from perceptual measurements (centroids from polar plots in each case) was approximately 20 degrees. These accuracies can be easily achieved manually by surgeons. In brief, similar to the selection of optimum orientations of toric IOLs,[36,37] it is conceivable to develop algorithms based on the aberrations of the eyes that guide clinicians to choose the optimum orientation of the IOL, which is similar to the ideal observer model approach described in this study. These should preferably use topography-based corneal aberrations as the crystalline lens is removed during the procedure. Alternatively, adaptive optics or simultaneous vision systems can be used to base the decision on perceptual measurement in patients, provided that the lens is not fully opacified by cataract.

In conclusion, we measured visual and perceptual performance to different orientations of a commercial bifocal design IOL at far, intermediate, and near distances. The HCVA did not differ much across orientations and distances. The perceptual performance and preferences were different across orientations and distances in most subjects. We show that these preferences are closely associated with the optical quality of the eye defined by the lower-order aberrations and HOAs. In the absence of modalities to customize the entire IOL design, small changes in the orientation of IOL implantation could result in improved perceptual quality. These preferences should be assessed before surgery, considering the visual needs of the patients and more important, each patient's optical quality.

### WHAT WAS KNOWN

- Computer and experimental visual simulations show that rotationally asymmetric IOL designs tend to provide better visual quality than concentric IOL designs.
- The predicted optical quality with angular designs varies with orientation and is affected by the subject's aberrations, in particular coma.
- Clinical studies of visual simulations show they do not affect IOL orientation overall, although there are some differences at the individual level.

### WHAT THIS PAPER ADDS

- Visual simulations of a rotationally asymmetric IOL at different orientations on the same patient showed consistent differences in perceived visual quality across orientations.
- Implanting a rotationally asymmetric IOL along the identified preferred orientation can optimize perceptual quality and visual performance.
- The preferred orientation was influenced by ocular optics and ocular and corneal aberrations, which can be used to predict the orientations in which the IOL should be implanted.

## REFERENCES

1. Charman WN. Developments in the correction of presbyopia II: surgical approaches. Ophthalmic Physiol Opt 2014; 34:397–426. Available at: http://onlinelibrary.wiley.com/doi/10.1111/opo.12129/epdf. Accessed July 11, 2016
2. Cochener B, Lafuma A, Khoshnood B, Courouve L, Berdeaux G. Comparison of outcomes with multifocal intraocular lenses: a meta-analysis. Clin Ophthalmol 2011; 5:45–56. Available at: http://www.ncbi.nlm.nih.gov/pmc/articles/PMC3033003/pdf/opth-5-045.pdf. Accessed July 11, 2016
3. de Gracia P, Dorronsoro C, Marcos S. Multiple zone multifocal phase designs. Opt Lett 2013; 38:3526–3529. Available at: http://

www.vision.csic.es/Publications/Articles/Multiple%20zone%20multifocal%20phase%20designs.pdf. Accessed July 11, 2016
4. Vinas M, Dorronsoro C, Gonzalez V, Cortes D, Radhakrishnan A, Marcos S. Testing vision with angular and radial multifocal designs using adaptive optics. Vision Res 2016 In press
5. Venter JA, Barclay D, Pelouskova M, Bull CEL. Initial experience with a new refractive rotationally asymmetric multifocal intraocular lens. J Refract Surg 2014; 30:770–776
6. Alió JL, Plaza-Puche AB, Montalban R, Javaloy J. Visual outcomes with a single-optic accommodating intraocular lens and a low-addition-power rotational asymmetric multifocal intraocular lens. J Cataract Refract Surg 2012; 38:978–985
7. Thomas BC, Auffarth GU, Philips R, Novák J, Blazek J, Adamkova H, Rabsilber TM. Klinische Ergebnisse nach Implantation einer neuen segmentalen refraktiven Multifokallinse [Clinical results after implantation of a new segmental refractive multifocal intraocular lens]. Ophthalmologe 2013; 110:1058–1062
8. Alio JL, Plaza-Puche AB, Javaloy J, Ayala MJ, Moreno LJ, Piñero DP. Comparison of a new refractive multifocal intraocular lens with an inferior segmental near add and a diffractive multifocal intraocular lens. Ophthalmology 2012; 119:555–563
9. Bala C, Meades K. Improvement in vision with inverted placement of an asymmetric refractive multifocal intraocular lens. J Cataract Refract Surg 2014; 40:833–835
10. de Wit DW, Diaz J, Moore TCB, Moutari S, Moore JE. Effect of position of near addition in an asymmetric refractive multifocal intraocular lens on quality of vision. J Cataract Refract Surg 2015; 41:945–955
11. Ramón ML, Piñero DP, Pérez-Cambrodí RJ. Correlation of visual performance with quality of life and intraocular aberrometric profile in patients implanted with rotationally asymmetric multifocal IOLs. J Refract Surg 2012; 28:93–99
12. Bonaque-González S, Ríos S, Amigó A, López-Gil N. Influence on visual quality of intraoperative orientation of asymmetric intraocular lenses. J Refract Surg 2015; 31:651–657
13. Piers PA, Fernandez EJ, Manzanera S, Norrby S, Artal P. Adaptive optics simulation of intraocular lenses with modified spherical aberration. Invest Ophthalmol Vis Sci 2004; 45:4601–4610. Available at: http://iovs.arvojournals.org/article.aspx?articleid=2163182. Accessed July 11, 2016
14. de Gracia P, Dorronsoro C, Gambra E, Marin G, Hernández M, Marcos S. Combining coma with astigmatism can improve retinal image over astigmatism alone. Vision Res 2010; 50:2008–2014
15. de Gracia P, Dorronsoro C, Sánchez-González A, Sawides L, Marcos S. Experimental simulation of simultaneous vision. Invest Ophthalmol Vis Sci 2013; 54:415–422. Available at: http://iovs.arvojournals.org/article.aspx?articleid=2188946. Accessed July 11, 2016
16. Dorronsoro Días C, Marcos Celestino S, inventors; Consejo Superior De Investigaciones Cientificas, assignee. Instrument for simulation of multifocal ophthalmic corrections.US patent 8 876 289. April 8, 2009. Available at: https://www.google.com/patents/US8876289. Accessed July 11, 2016
17. Juday RD. Correlation with a spatial light modulator having phase and amplitude cross coupling. Appl Opt 1989; 28:4865–4869
18. Brainard DH. The psychophysics toolbox. Spat Vis 1997; 10:433–436
19. Wanders BFM, inventor; Procornea Holding B.V., applicant. Intraocular lens. Netherlands patent PCT/NL2013/050013. January 11, 2012. Available at: https://google.com/patents/WO2013105855A1?cl=en. Accessed July 11, 2016
20. Marcos S, Burns SA. On the symmetry between eyes of wavefront aberration and cone directionality. Vision Res 2000; 40:2437–2447
21. Radhakrishnan A, Dorronsoro C, Sawides L, Marcos S. Short-term neural adaptation to simultaneous bifocal images. PLoS One 2014; 9:e93089. Available at: http://journals.plos.org/plosone/article/asset?id=10.1371%2Fjournal.pone.0093089.PDF. Accessed July 11, 2016
22. Grosvenor T. Primary Care Optometry, 3rd ed. Boston, MA, Butterworth-Heinemann, 1996; 309–340
23. Ehrenstein WH, Ehrenstein A. Psychophysical methods. In: Windhorst U, Johansson H, eds, Modern Techniques in Neuroscience Research. Berlin, Germany, Springer Verlag, 1999; 1211–1240
24. Marcos S, Sawides L, Gambra E, Dorronsoro C. Influence of adaptive-optics ocular aberration correction on visual acuity at different luminances and contrast polarities. J Vis 2008; 8:1–12. Available at: http://www.journalofvision.org/8/13/1/. Accessed July 11, 2016
25. Iskander DR. Computational aspects of the visual Strehl ratio. Optom Vis Sci 2006; 83:57–59. Available at: http://journals.lww.com/optvissci/Fulltext/2006/01000/Computational_Aspects_of_the_Visual_Strehl_Ratio.15.aspx. Accessed July 11, 2016
26. Vaz TC, Gundel RE. High- and low-contrast visual acuity measurements in spherical and aspheric soft contact lens wearers. Cont Lens Anterior Eye 2003; 26:147–151
27. Rouger H, Benard Y, Legras R. Effect of monochromatic induced aberrations on visual performance measured by adaptive optics technology. J Refract Surg 2010; 26:578–587
28. Winn B, Whitaker D, Elliott DB, Phillips NJ. Factors affecting light-adapted pupil size in normal human subjects. Invest Ophthalmol Vis Sci 1994; 35:1132–1137. Available at: http://iovs.arvojournals.org/article.aspx?articleid=2161149. Accessed July 11, 2016
29. Blakemore C, Campbell FW. On the existence of neurones in the human visual system selectively sensitive to the orientation and size of retinal images. J Physiol 1969; 203:237–260. Available at: http://www.ncbi.nlm.nih.gov/pmc/articles/PMC1351526/pdf/jphysiol01073-0239.pdf. Accessed July 11, 2016
30. Bosking WH, Zhang Y, Schofield B, Fitzpatrick D. Orientation selectivity and the arrangement of horizontal connections in tree shrew striate cortex. J Neurosci 1997; 17:2112–2127. Available at: http://www.jneurosci.org/content/17/6/2112.full.pdf. Accessed July 11, 2016
31. Ohlendorf A, Tabernero J, Schaeffel F. Neuronal adaptation to simulated and optically-induced astigmatic defocus. Vision Res 2011; 51:529–534
32. Vinas M, de Gracia P, Dorronsoro C, Sawides L, Marin G, Hernández M, Marcos S. Astigmatism impact on visual performance: meridional and adaptational effects. Optom Vis Sci 2013; 90:1430–1442. Available at: http://journals.lww.com/optvissci/Fulltext/2013/12000/Astigmatism_Impact_on_Visual_Performance__.13.aspx. Accessed July 11, 2016
33. Yehezkel O, Sagi D, Sterkin A, Belkin M, Polat U. Learning to adapt: dynamics of readaptation to geometrical distortions. Vision Res 2010; 50:1550–1558
34. Sawides L, Dorronsoro C, de Gracia P, Vinas M, Webster M, Marcos S. Dependence of subjective image focus on the magnitude and pattern of high order aberrations. J Vis 2012; 12:1–12. Available at: http://jov.arvojournals.org/article.aspx?articleid=2192226. Accessed July 11, 2016
35. Sawides L, de Gracia P, Dorronsoro C, Webster M, Marcos S. Adapting to blur produced by ocular high-order aberrations. J Vis 2011; 11:1–11. Available at: http://www.ncbi.nlm.nih.gov/pmc/articles/PMC3244874/pdf/nihms344261.pdf. Accessed July 11, 2016

36. Ma JJK, Tseng SS. Simple method for accurate alignment in toric phakic and aphakic intraocular lens implantation. J Cataract Refract Surg 2008; 34:1631–1636
37. Buckhurst PJ, Wolffsohn JS, Davies LN, Naroo SA. Surgical correction of astigmatism during cataract surgery. Clin Exp Optom 2010; 93:409–418. Available at: http://onlinelibrary.wiley.com/doi/10.1111/j.1444-0938.2010.00515.x/epdf. Accessed July 11, 2016

## OTHER CITED MATERIAL

A. Dorronsoro C, Radhakrishnan A, de Gracia P, Sawides L, Ramón Alonso-Sanz J, Cortés D, Marcos S, "Visual Testing of Segmented Bifocal Corrections With a Compact Simultaneous Vision Simulator," presented at the annual meeting of the Association for Research in Vision and Ophthalmology, Orlando, Florida, USA, May 2014. ARVO E-Abstract 55. Available at: http://iovs.arvojournals.org/article.aspx?articleid=2272300. Accessed July 11, 2016
B. Radhakrishnan A, Dorronsoro C, Marcos S, "Adaptation to Optical Simulation of Simultaneous Bifocal Vision," presented at the annual meeting of the Association for Research in Vision and Ophthalmology, Denver, Colorado, USA, May 2015. Abstract Available at: http://iovs.arvojournals.org/article.aspx?articleid=2332722. Accessed July 11, 2016
C. Montelongo Y, Palani A, Wilkinson T, "Simulations of Time Multiplexed Fraunhofer Holograms Produced by Binary Phase SLMs for Video Projection," presented at the Latin America Optics and Photonics Conference, Sao Sebastiao, Brazil, November 2012

First author:
Aiswaryah Radhakrishnan, MPhil

*Laboratory of Visual Optics and Biophotonics, Instituto de Óptica Daza de Valdés, Consejo Superior de Investigaciones Científicas, Madrid, Spain*